

Study of the solar wind-magnetosphere coupling on different time scales

Badruddin and O. P. M. Aslam

*Department of Physics, Aligarh Muslim University, Aligarh-202002, India.
e-mail: badr.physamu@gmail.com*

ABSTRACT

Solar wind-magnetosphere coupling, its causes and consequences have been studied for the last several decades. However, the assessment of continuously changing behaviour of the sun, plasma and field flows in the interplanetary space and their influence on geomagnetic activity is still a subject of intense research. Search for the best possible coupling function is also important for space weather prediction. We utilize four geomagnetic indices (*ap*, *aa*, *AE* and *Dst*) as parameters of geomagnetic activity level in the earth's magnetosphere. In addition to these indices, we utilize various solar wind plasma and field parameters for the corresponding periods. We analyse the geomagnetic activity and plasma/field parameters at yearly, half-yearly, 27-day, daily, 3-hourly, and hourly time resolutions. Regression analysis using geomagnetic and solar wind data of different time resolutions, over a continuous long period, and at different phases of solar activity (increasing including maximum/decreasing including minimum) led us to suggest that two parameters $BV/1000$ (mV m^{-1}) and BV^2 (mV s^{-1}) are highly correlated with the all four geomagnetic activity indices not only at any particular time scale but at different time scales. It probably suggests for some role of the fluctuations/variability in interplanetary electric potential, its spacial variation [i.e., interplanetary electric field BV (mV m^{-1})] and/or time variation [BV^2 (mV s^{-1})], in influencing the reconnection rate.

Keywords: Solar wind-magnetosphere coupling, Interplanetary electric field, Geomagnetic activity, Space weather prediction

1. Introduction

In the area of solar-terrestrial physics, one of the key problems is to investigate the mechanism of energy transfer from the solar wind into the magnetosphere. Another related key issue is to investigate the mechanism that excites magnetic disturbances in the geo-magnetosphere. It is generally believed that the basic parameter leading to geomagnetic disturbances is the southward component of the interplanetary magnetic field ($-B_z$) and/or the duskward component of the interplanetary electric field $E_y = -V_x B_z$ (see, e.g., Dungey, 1961; Rostoker and Fälthammar, 1967; Burton et al., 1975; Akasofu, 1981; Badruddin, 1998; Echer et al., 2005; Gopalswamy et al., 2008; Badruddin and Singh, 2009; Alves et al., 2011; Guo et al., 2011; Singh and Badruddin, 2012; Yermolaev et al., 2012 and references therein). With negative B_z , reconnection occurs at the daytime magnetopause between the Earth's magnetic field and southward B_z component of the interplanetary magnetic field (Kane, 2010). The principal manifestation of geomagnetic storms, measured by the index *Dst*, is the increase of ring current intensity, which depends upon the reconnection rate.

Origin of the intense southward magnetic fields are the interplanetary shock/sheath region, coronal mass ejections/magnetic clouds, stream interaction regions etc. (e.g., Lepping et al., 1991; Märcz, 1992; Tsurutani and Gonzalez, 1997; Richardson et al., 2000; Webb et al., 2000; Kudela and Storini, 2005; Kim et al., 2005; Gopalswamy et al., 2007; Singh and Badruddin, 2007; Zhang et al., 2007; Gupta and Badruddin, 2009; Yermolaev et al., 2010; Alves et al., 2011; Mustajab and Badruddin, 2011; Richardson and Cane, 2011; Kudela, 2013) and arrival of these structures leads to changes/fluctuations in various interplanetary plasma and field parameters.

In spite of the success of the so called Dungey mechanism (Arnoldy, 1971; Burton et al., 1975; Holzer and Slavin, 1979; Alves et al., 2011) some effort (e.g., Baker et al., 1981; Clauer et al., 1981; Holzer and Slavin, 1982; Murayama, 1982; Zhang and Burlaga, 1988; Papitashvili et al., 2000; Sabbah, 2000; Gupta and Badruddin, 2009; Dwivedi et al., 2009; Joshi et al., 2011) has gone into looking for other parameters that might correlate better with geomagnetic activity.

Geomagnetic activity being influenced by total interplanetary electric field (Papitashvili et al., 2000; Sabbah, 2000), irregularities in the solar wind and interplanetary magnetic field (Dessler and Fejer, 1963; Garrett et al., 1974; Crooker et al., 1977; Kershengolts et al., 2007), and enhanced dynamic pressure (Murayama, 1982; Srivastava and Venkatakrishnan, 2002; Boudouridis et al., 2005; Xie et al., 2008; Ontiveros and Gonzalez-Esparza, 2010; Singh and Badruddin, 2012) have been suggested. However, a unique relationship is still lacking which may ultimately lead to understand the intensity of geomagnetic disturbances.

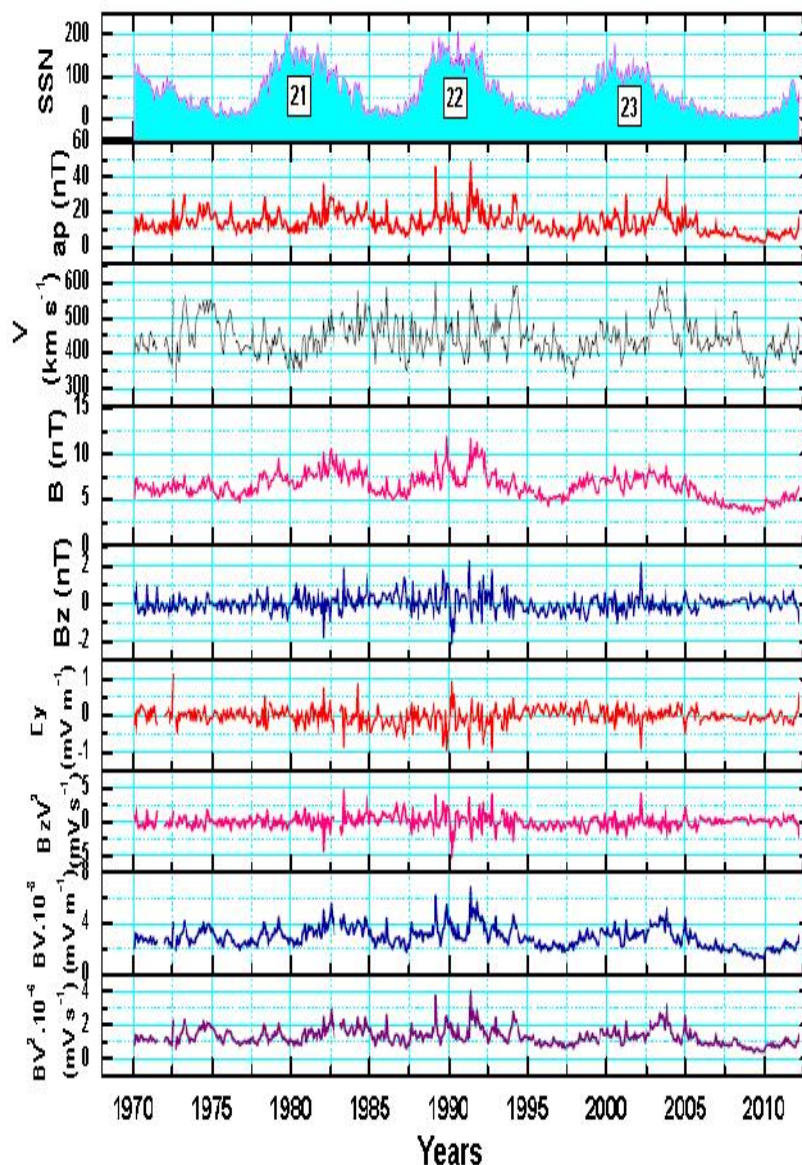


Fig. 1. Time variation of 27-day average solar (SSN), geomagnetic (ap), interplanetary plasma/field parameters V (km s^{-1}), B (nT), B_z (nT), E_y (mV m^{-1}), $B_z V^2$ (mV s^{-1}) and BV^2 (mV s^{-1}).

Most of the earlier efforts to search for better coupling functions, in general used one geomagnetic index or the other, at one time resolution or the other. Further, earlier studies were mainly focused over the durations of moderate to strong geomagnetic disturbances. To the best of our knowledge, none of the previous correlative studies were done over extended periods of several solar cycles using different geomagnetic activity and solar wind parameters at multiple time resolutions. In this work we analyse the continuous data for long periods (~40 years), that contain quiet, weak, moderate as well as strong geomagnetic activity periods. In this paper, we present the results of the analysis using interplanetary plasma and field data and their various derivatives together with various geomagnetic indices of different time resolutions; yearly, half-yearly, 27-day, daily, 3-hourly and hourly resolutions.

2. Results and Discussion

In Fig. 1, we have plotted the time variation of 27-day average solar, geomagnetic and interplanetary parameters (<http://omniweb.gsfc.nasa.gov>) for more than three solar cycles (1970-2011). The parameters

plotted in this figure are; sunspot number (SSN) -a solar activity parameter; *ap* index -a parameter of geomagnetic activity; interplanetary plasma and field parameters -solar wind velocity *V* (km s⁻¹), interplanetary magnetic field *B* (nT), its north-south component *B_z* (nT), duskward electric field *E_y* (mV m⁻¹), ‘spacial variation of interplanetary electric potential’ i.e., the interplanetary electric field *BV*.10⁻³ (mV m⁻¹), and two more derivatives that may be referred as ‘time variation of the duskward electric potential’ *BzV²* (mV s⁻¹), and the ‘time variation of total interplanetary electric potential’ *BV²* (mV s⁻¹); although suitability of these latter nomenclatures need to be confirmed. From Fig. 1 alone, it is difficult to infer about interplanetary plasma/field parameter whose time variation best matches with time variation in geomagnetic activity level, it looks, however, as if the time variation of *BV²* is relatively better related to *ap* variations at this (27-day average) time resolution.

In order to understand the response of magnetosphere to varying interplanetary conditions, attempts have been made in the past to search for the parameter(s) that can best explain the occurrence of geomagnetic disturbances, but, efforts are needed to find a relationship that may ultimately lead to unambiguously understand the solar wind-magnetosphere coupling and disturbances in the geomagnetosphere.

As solar polarity reverses at/near each solar activity maximum, we have divided a complete solar cycle into two parts; (i) increasing including maximum and (ii) decreasing including minimum phases. This division is aimed to look for, if any, the large-scale interplanetary magnetic field (IMF) polarity dependent effects of solar plasma/field parameters on the geomagnetic activity. It is to be mentioned here

that large scale IMF-polarity is positive (outward above the heliospheric current sheet and inward below the heliospheric current sheet) during decreasing including minimum phases and negative (inward above the heliospheric current sheet and outward below the heliospheric current sheet) during increasing including maximum phases of even solar cycles (e.g., solar cycles 20 and 22), opposite will be the polarity during similar phases of odd solar cycles (e.g., solar cycles 21 and 23).

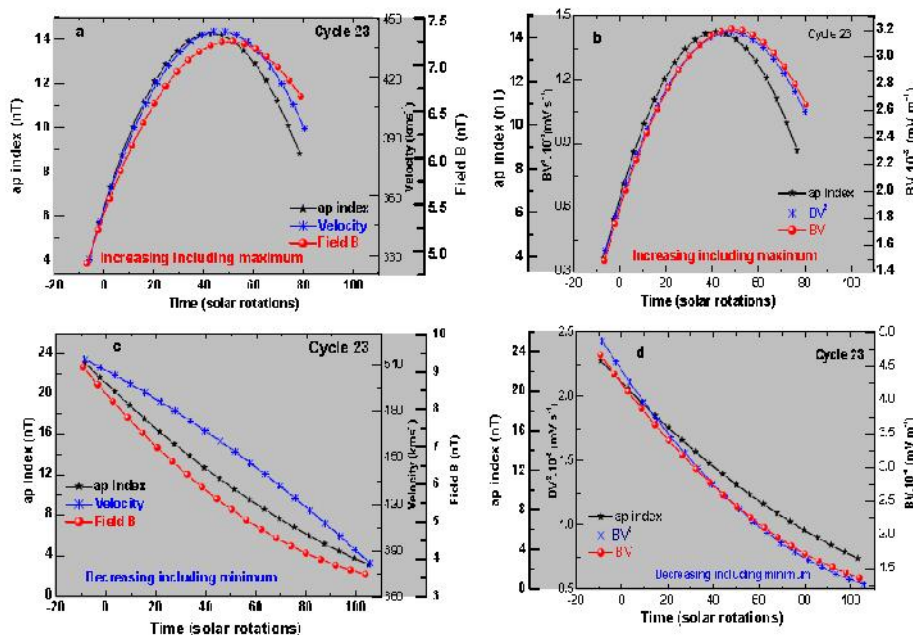


Fig. 2. Best-fit polynomial curves ($y = A+B_1x+B_2x^2$) for different interplanetary parameters and geomagnetic parameter *ap* during (a and b) increasing including maximum and (c and d) decreasing including minimum of solar cycle 23.

We have adopted two approaches, (a) best-fit approach and (b) correlative analysis approach. First, we did the polynomial ($y = A+B_1x+B_2x^2$) fit to the 27-day averaged parameters (*ap*, *B*, *B_z*, *B_zV*, *V*, *P*, *E_y*, *BV*, *BzV²* and *BV²*), both during (i) increasing including maximum phase and (ii) decreasing including minimum phase of solar cycle 23. The constants *B₁*, *B₂* and determination coefficient (*R²*) for the best-fit curves to the time evolutions of different parameters during both the phases of cycle 23 are given in Table 1. We can see from the values of *R²* that the polynomial fit is not good for all parameters. It is relatively better in case of interplanetary parameters *B*, *V*, *BV* and *BV²*. In order to see which of these

parameters better follows the polynomial fitted curve of geomagnetic parameter ap , we have plotted them in Fig. 2. From these fitted curves, it is difficult to make any clear distinction between various plasma/field parameters (B , V , BV and BV^2) as regards to which of them tracks relatively better the time evolution of geomagnetic activity parameter ap .

Table 1 Best fit parameters B_1 and B_2 and determination coefficient (R^2) obtained by fitting polynomial ($y = A + B_1x + B_2x^2$) to the time evolution of different parameters (27-day average data) during different phases solar cycle 23.

Parameters	Decreasing including minimum phase			Increasing including maximum phase		
	B_1	B_2	R^2	B_1	B_2	R^2
ap index (nT)	-0.24 ± 0.07	$(6.2 \pm 6.7) \times 10^{-4}$	0.55	0.36 ± 0.10	-0.004 ± 0.001	0.19
B (nT)	-0.08 ± 0.002	$(2.8 \pm 0.78) \times 10^{-4}$	0.87	0.07 ± 0.02	$-(7.2 \pm 2.0) \times 10^{-4}$	0.38
B_z (nT)	0.002 ± 0.004	$(6.3 \pm 4.2) \times 10^{-4}$	0.08	0.006 ± 0.01	$(1.8 \pm 1.5) \times 10^{-4}$	0.08
Sigma B (nT)	-0.002 ± 0.01	$-(1.8 \pm 0.97) \times 10^{-4}$	0.42	0.03 ± 0.02	$-(2.5 \pm 2.2) \times 10^{-4}$	0.09
V (km s $^{-1}$)	-0.87 ± 0.7	-0.003 ± 0.007	0.32	3.87 ± 0.66	-0.04 ± 0.009	0.39
P (n Pa)	-8.65 ± 0.005	$-(1.2 \pm 4.8) \times 10^{-4}$	0.54	-0.01 ± 0.007	$(8.8 \pm 9.7) \times 10^{-5}$	0.02
E_y (mV m $^{-1}$)	$-4.1 \times 10^{-4} \pm 0.002$	$(1.02 \pm 1.95) \times 10^{-5}$	0.09	-0.002 ± 0.005	$-(2.1 \pm 6.3) \times 10^{-5}$	0.09
$B_z V^2 \cdot 10^{-5}$ (mV s $^{-1}$)	-0.007 ± 0.01	$-(5.14 \pm 9.9) \times 10^{-6}$	0.07	-0.003 ± 0.02	$(1.66 \pm 2.72) \times 10^{-4}$	0.05
$BV^2 \cdot 10^{-6}$ (mV s $^{-1}$)	-0.03 ± 0.005	$-(9.88 \pm 5.3) \times 10^{-5}$	0.63	0.034 ± 0.006	$-(3.54 \pm 0.74) \times 10^{-5}$	0.43
$BV \cdot 10^{-3}$ (mV m $^{-1}$)	-0.04 ± 0.007	$-(1.57 \pm 0.67) \times 10^{-4}$	0.77	0.06 ± 0.009	$-(5.7 \pm 1.2) \times 10^{-4}$	0.45

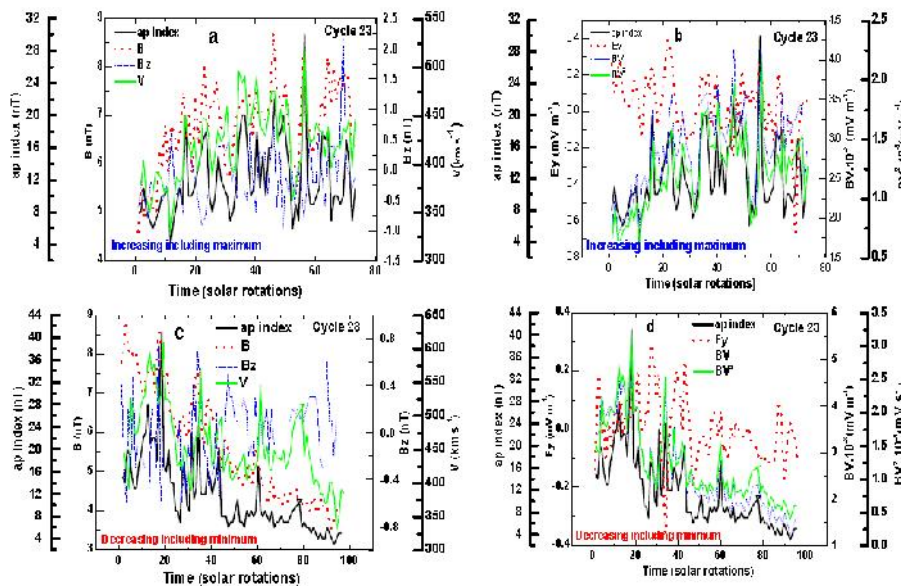


Fig. 3. Time variation (27-day solar rotation average) of various interplanetary plasma/field parameters with geomagnetic ap index during increasing including maximum (a and b) and decreasing including minimum (c and d) phases of solar cycle 23.

Therefore, as a next step, we have considered the time variations in different parameters at this time scale (27-day), both during increasing including maximum and decreasing including minimum phases of solar cycle 23. These time variations in various interplanetary plasma/field parameters (V , B ,

B_z , E_y , BV and BV^2) are compared with time variations of geomagnetic parameter ap (see Fig. 3 (a-d)). From these figures, it appears that, at this time scale, BV and BV^2 follow better the time variation of ap , as compared to other parameters V , B , B_z and E_y considered here.

Table 2a
 Rate of change of the ap index with various parameters ($\Delta I/\Delta P$) and correlation coefficient (R) during increasing including maximum phases of solar cycles 20, 21, 22 and 23 using 27-day average data.

Parameters	Solar cycle 20		Solar cycle 21		Solar cycle 22		Solar cycle 23	
	$\Delta I/\Delta P$	R	$\Delta I/\Delta P$	R	$\Delta I/\Delta P$	R	$\Delta I/\Delta P$	R
B (nT)	3.44±0.67	0.57	2.81±0.54	0.55	3.99±0.45	0.74	3.77±0.48	0.68
B_z (nT)	-3.44±1.0	-0.42	-1.32±1.34	-0.13	-3.08±1.35	-0.28	-2.65±1.09	-0.29
Sigma B (nT)	3.3±0.86	0.46	3.08±0.80	0.44	4.87±0.76	0.62	4.17±0.53	0.68
V (km s ⁻¹)	0.08±0.01	0.69	0.10±0.01	0.78	0.12±0.01	0.77	0.10±0.01	0.77
P (n Pa)	8.08±1.35	0.35	5.41±1.06	0.54	7.43±0.67	0.80	7.62±1.43	0.53
E_y (mV m ⁻¹)	9.38±1.62	0.61	2.3±2.82	0.10	5.76±2.93	0.24	6.27±2.46	0.29
$B_z V^2 \cdot 10^5$ (mV s ⁻¹)	-1.80±0.52	-0.42	-0.83±0.73	-0.14	-1.34±0.63	-0.25	-1.72±0.56	-0.34
$BV^2 \cdot 10^4$ (mV s ⁻¹)	11.4±1.32	0.77	11.4±1.02	0.82	18.53±0.72	0.90	12.01±0.93	0.84
$BV \cdot 10^3$ (mV m ⁻¹)	7.3±0.84	0.76	6.35±0.68	0.76	7.38±0.51	0.87	7.0±0.60	0.81

The plots in Fig. 3 provide only a qualitative idea about the time variations of various plasma/field parameters as compared to geomagnetic parameter ap during (a) increasing including maximum and (b) decreasing including minimum phase of solar cycle 23. Therefore, a quantitative analysis has been done by best-fit linear regression analysis, not only during (a) increasing including maximum and (b) decreasing including minimum phase of solar cycle 23, and but also during similar phases of solar cycles 20, 21 and 22. The rate of change of the ap index with various plasma/field parameters (I/P) obtained from the best-fit method and linear correlation coefficients between them are tabulated in Table 2a during increasing including maximum phases of solar cycles 20, 21, 22 and 23. From this table we observe that, out of various plasma/field parameters, the correlations are found to be best with parameters BV (mV m⁻¹) or BV^2 (mV s⁻¹), consistently during increasing including maximum phases of all four solar cycles 20, 21, 22 and 23, at this time resolution (27-day) of the data. The scatter plot and best-fit linear curves of ap with BV and BV^2 are shown in Fig. 4a and Fig. 4c.

Table 2b
 Rate of change of the ap index with various parameters ($\Delta I/\Delta P$) and correlation coefficient (R) during decreasing including minimum phases of solar cycles 20, 21, 22 and 23 using 27-day average data.

Parameters	Solar cycle 20		Solar cycle 21		Solar cycle 22		Solar cycle 23	
	$\Delta I/\Delta P$	R	$\Delta I/\Delta P$	R	$\Delta I/\Delta P$	R	$\Delta I/\Delta P$	R
B (nT)	4.20±0.69	0.54	3.08±0.33	0.76	2.62±0.42	0.60	3.76±0.26	0.83
B_z (nT)	2.10±1.69	0.14	-3.85±1.29	-0.37	0.03±1.21	0.003	-6.47±2.20	-0.31
Sigma B (nT)	3.6±0.77	0.44	4.43±0.69	0.63	3.02±0.58	0.54	5.86±0.53	0.75
V (km s ⁻¹)	0.07±0.01	0.78	0.07±0.01	0.53	0.06±0.009	0.64	0.09±0.007	0.81
P (n Pa)	6.83±1.16	0.55	4.89±1.22	0.46	6.99±1.01	0.65	10.7±1.89	0.77
E_y (mV m ⁻¹)	-0.73±3.72	-0.02	7.2±2.56	0.34	0.56±2.67	0.03	14.8±4.85	0.30
$B_z V^2 \cdot 10^5$ (mV s ⁻¹)	1.22±0.81	0.16	-1.25±0.59	-0.26	0.19±0.58	0.04	-2.77±0.96	-0.29
$BV^2 \cdot 10^4$ (mV s ⁻¹)	11.2±0.72	0.85	10.8±0.84	0.86	94.2±0.89	0.79	11.31±0.44	0.93
$BV \cdot 10^3$ (mV m ⁻¹)	7.8±0.58	0.83	6.51±0.48	0.87	5.98±0.59	0.78	6.5±0.30	0.92

Similar correlative analysis during decreasing including minimum phases of solar cycles 20, 21, 22 and 23 were also done; the values of the rate of change of geomagnetic index ap with various parameters (I/P) and correlation coefficients are tabulated in Table 2b. From Table 2b, we observe that out of all

parameters considered here, the BV and BV^2 are correlated better with the ap during decreasing including minimum phases of almost all the four cycles 20, 21, 22 and 23 averaged over the solar rotation time scale. The scatter plots with best-fit curve during decreasing including minimum phase of all four cycles are shown in Fig. 4b and Fig. 4d. A comparison of the values of I/P and R in Table 2a and Table 2b does not show any large-scale IMF-polarity dependent change in these values.

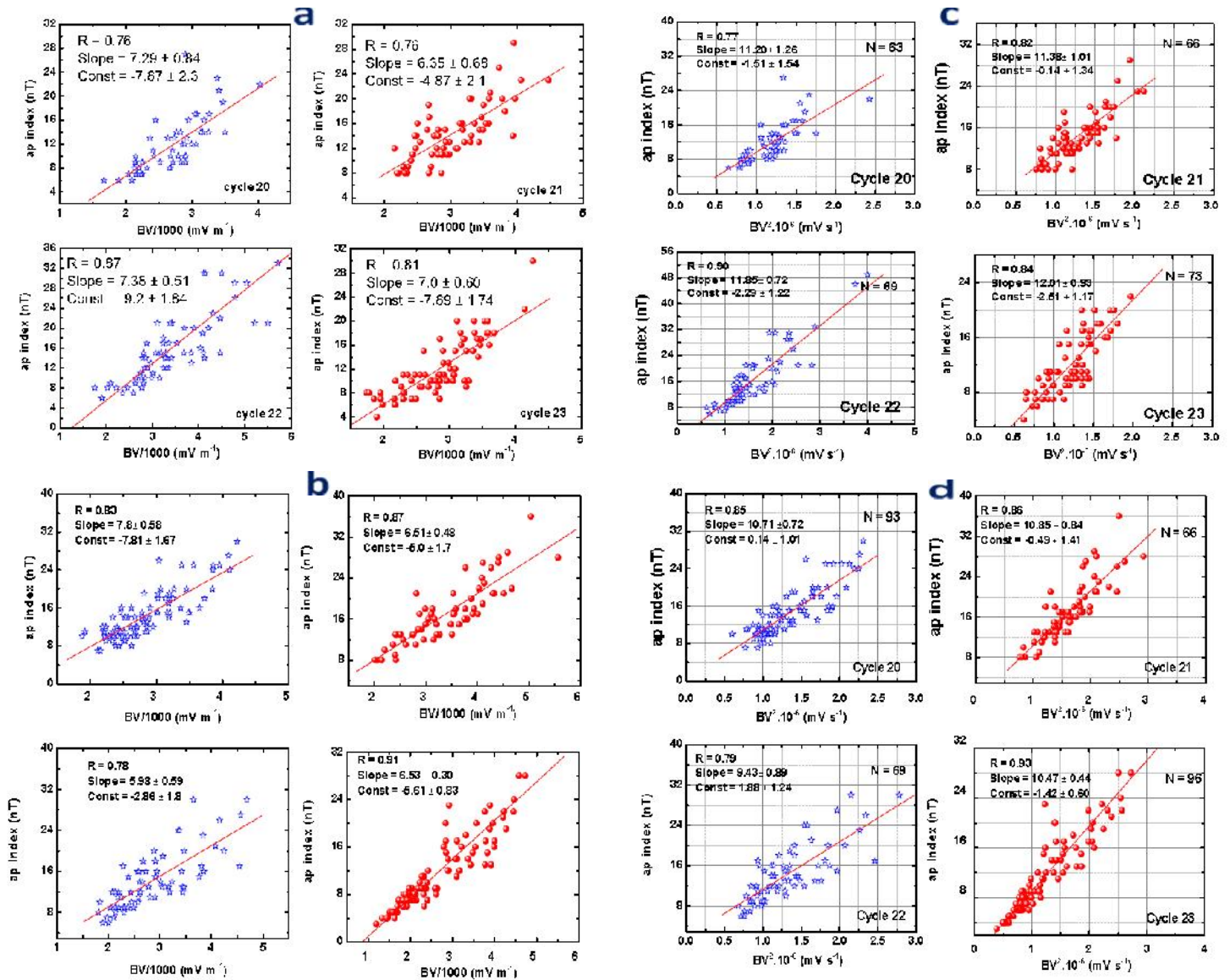


Fig. 4. (a) Scatter plot with best-fit linear curve between ap and BV during increasing including maximum period of different solar cycles (20 – 23). (b) Scatter plot with the best-fit linear curve between ap and BV during decreasing including minimum period of different solar cycles (20 – 23). (c) Scatter plot with best-fit linear curve between ap and BV^2 during increasing including maximum period of different solar cycles (20 – 23). (d) Scatter plot with the best-fit linear curve between ap and BV^2 during decreasing including minimum period of different solar cycles (20 – 23).

As we do not see any major difference in the values of I/P during different solar cycles, as a next step, to find the best relation between geomagnetic indices and plasma/field parameters, we have combined the data of all four solar cycles during (a) increasing including maximum and (b) decreasing including minimum phases of solar cycles and did regression analysis of the combined data. To see the consistency we did a similar analysis with another geomagnetic index (aa) (<http://ftp.ngdc.noaa.gov>) also. The scatter plots of geomagnetic parameters (aa and ap) with BV and BV^2 for (i) increasing including maximum

phase [Fig. 5 (a and b), Fig. 6 (a and b)], (ii) decreasing including minimum phase [Fig. 5 (c and d), Fig. 6 (c and d)] and (iii) combined periods [Fig. 5 (e and f), Fig. 6 (e and f)] with values of I/P and R are shown in Fig. 5 and Fig. 6. From these figures, we can give best-fit relationship for solar rotation averaged data as follows:

$$\begin{aligned} ap &= 6.72 \times 10^{-3} (BV) - 5.94 \\ ap &= 1.10 \times 10^{-5} (BV^2) - 0.83 \\ aa &= 8.77 \times 10^{-3} (BV) - 2.87 \\ aa &= 1.45 \times 10^{-5} (BV^2) + 3.56 \end{aligned}$$

We have analysed and discussed the results based on the solar-rotation (27-day) averaged data. However, as shown in Fig. 7 (a, b and c), there are distinct fluctuations in the time variability of parameters at different time averages; 27-day solar rotation average [Fig. 7 (a)], 1 day (daily) average [Fig. 7 (b)] and 1 hour (hourly) average [Fig. 7 (c)] data, plotted for solar cycle 23. We, therefore, performed correlation analyses using not only the solar cycle 23 data (most complete data as compared to previous cycles 20, 21 and 22) but also data for extended period (1970-2011) at various (yearly, half-yearly, 27-day, daily, 3-hourly and hourly) time resolutions. The calculated values of linear correlation coefficients (R) between geomagnetic parameter ap and various plasma/field parameters are given in Table 3a.

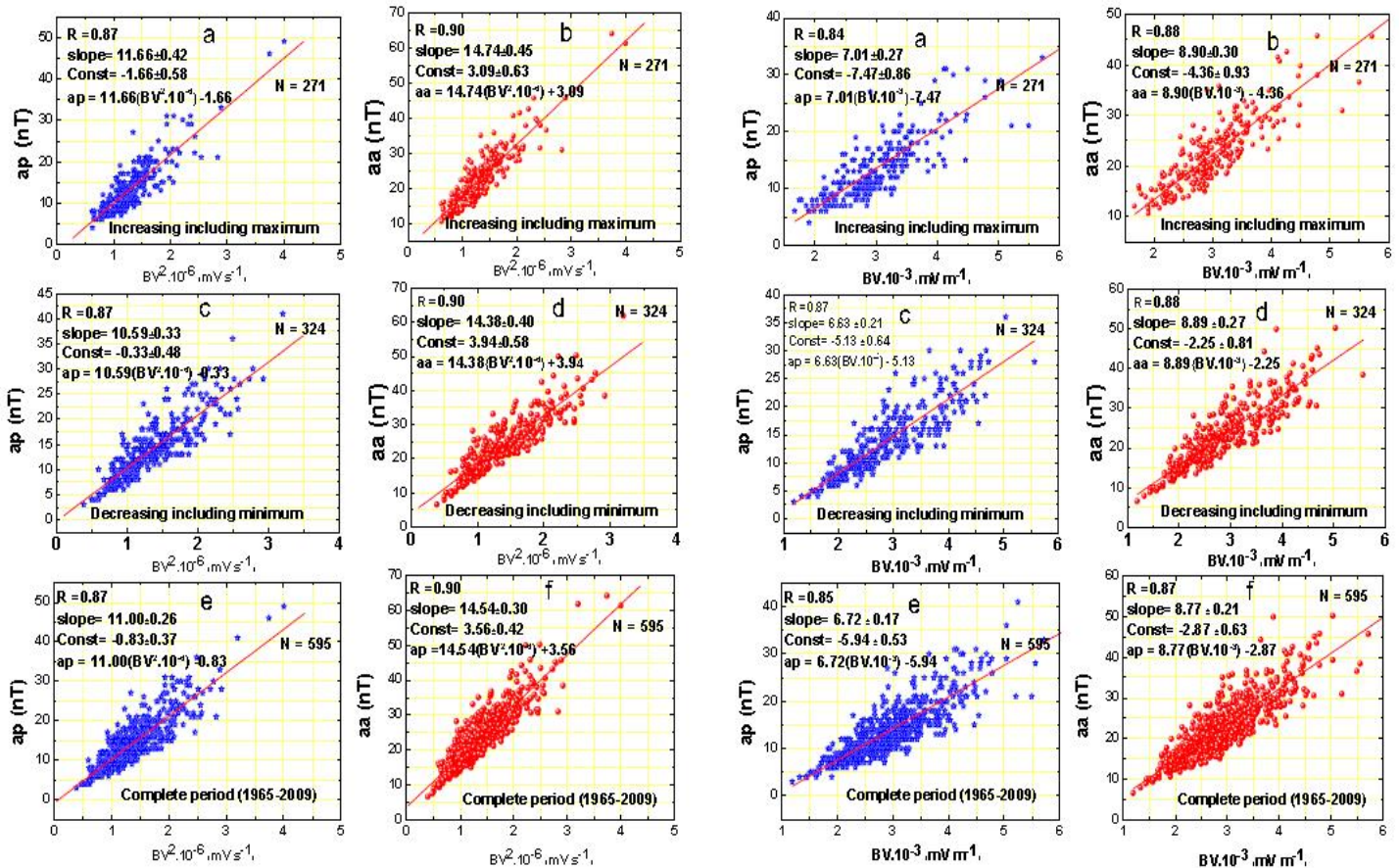


Fig. 5. Scatter plot and the best-fit linear curve between ap , aa and BV during (i) increasing including maximum phases (a and b), (ii) decreasing including minimum (c and d) phases and (iii) complete cycles (e and f) 20-23 combined.

Fig. 6. Scatter plot and best-fit linear curve between ap , aa and BV^2 during (i) increasing including maximum phases (a and b), (ii) decreasing including minimum (c and d) phases and (iii) complete cycles (e and f) 20-23 combined

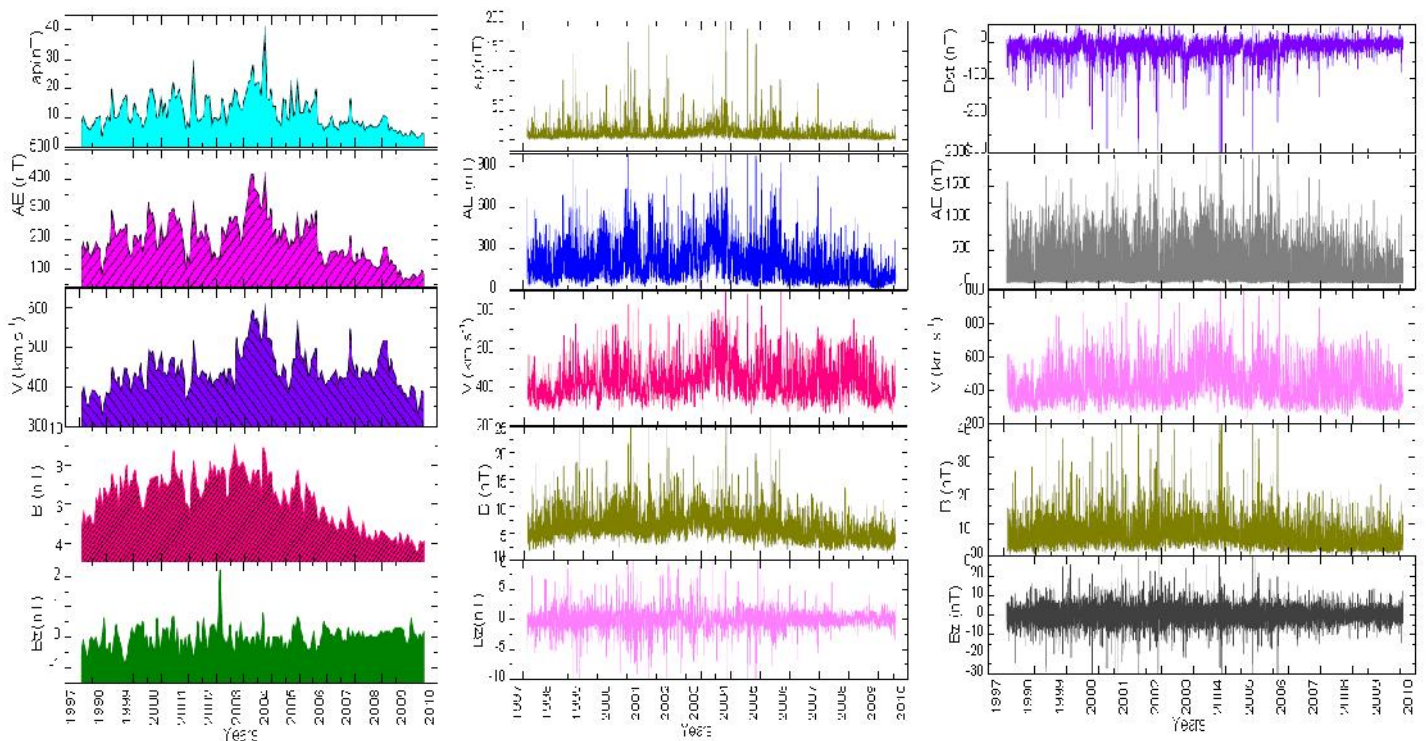


Fig. 7. (a) Time variation (27-day average) of various parameters during solar cycle 23. (b) Time variation (daily values) of various parameters during solar cycle 23. (c) Time variation (hourly values) of various parameters during solar cycle 23.

From this table we can see that, in general, for almost all the time resolutions of data (yearly, half-yearly, 27-day, daily and 3-hourly), BV and BV^2 are highly correlated with geomagnetic parameter ap . We have further extended our correlation analysis at various time scales to some other geomagnetic parameters; aa , AE and Dst (see Table 3 (b-d)). Again, we find that aa , AE and Dst are also better correlated with BV and BV^2 at almost all time resolutions (yearly, half-yearly, 27-day, daily, 3-hourly and hourly). Looking at the linear correlation coefficients (R) in Table 3a-d at various time resolutions, we see that the values of R for geomagnetic indices versus B_z (and also with E_y) are consistent at daily, 3-hourly and hourly time resolutions for all four periods considered; (1) increasing including maximum (2) decreasing including minimum (3) complete solar cycle 23 and (4) extended period 1970-2011. However, the value of R is of different sign (positive/negative) during increasing including maximum as compared to decreasing including minimum periods, at yearly and half-yearly time resolutions. This difference probably arises due to longer time averaging the parameters ($-B_z$ and E_y) which have both positive and negative values.

The relationships of geomagnetic parameters with BV and BV^2 are shown in Fig. 8 (a-d) and Fig. 9 (a-d) at various time resolutions. The equations obtained by the best-fit method are summarized in Table 4.

It is known that the primary interplanetary cause of moderate and intense geomagnetic storms is the presence of a southward interplanetary field structure in the solar wind and duskward electric field (E_y) is a crucial parameter. However, some other ‘preconditions’ playing an additional role in ‘influencing’ the magnetic reconnection rate and further enhancing the energy transfer from the solar wind to the magnetosphere has also been studied by earlier workers.

In early, 1960’s Snyder et al. (1963) showed that the geomagnetic activity Kp responds well to solar wind velocities (V). Rossberg (1989) used continues data of about six months to study the effect of solar wind velocity on substorm activity using the AL index. He observed that at high solar wind velocities, the

magnetic activity starts to increase already in the positive B_z range and that this result poses strong constraints on the generally accepted reconnection/merging model.

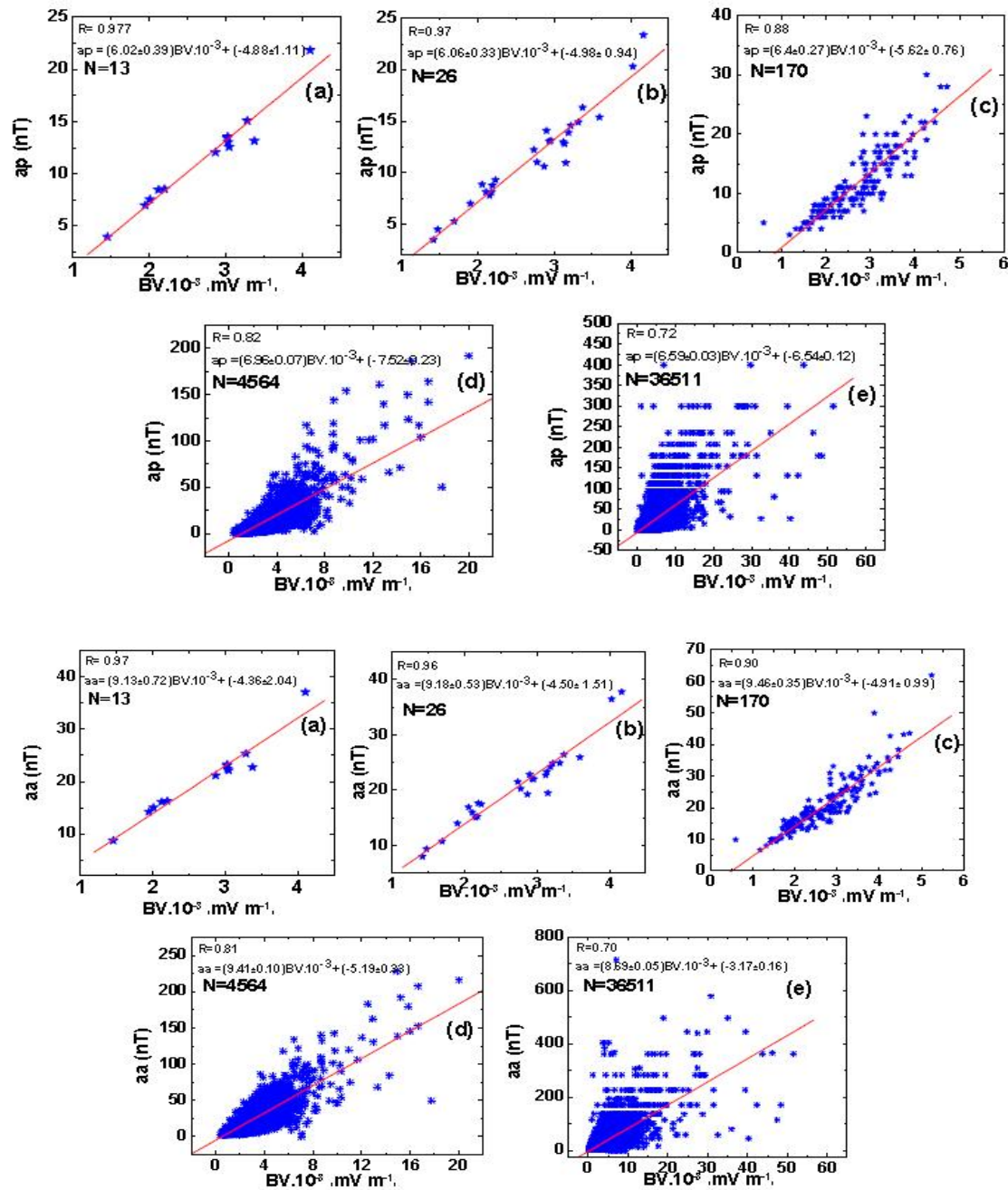


Fig. 8. (A) Scatter plot and best-fit linear curve between geomagnetic index ap and BV at different time resolutions; (a) yearly, (b) half-yearly, (c) 27-day, (d) daily and (e) 3-hourly. (B) Scatter plot and best-fit linear curve between geomagnetic index aa and BV at different time resolutions; (a) yearly, (b) half-yearly, (c) 27-day, (d) daily and (e) 3-hourly. (C) Scatter plot and best-fit linear curve between geomagnetic index AE and BV at different time resolutions; (a) yearly, (b) half-yearly, (c) 27-day, (d) daily, (e) 3-hourly and (f) hourly. (D) Scatter plot and best-fit linear curve between geomagnetic index Dst and BV at different time resolutions; (a) yearly, (b) half-yearly, (c) 27-day, (d) daily, (e) 3-hourly and (f) hourly.

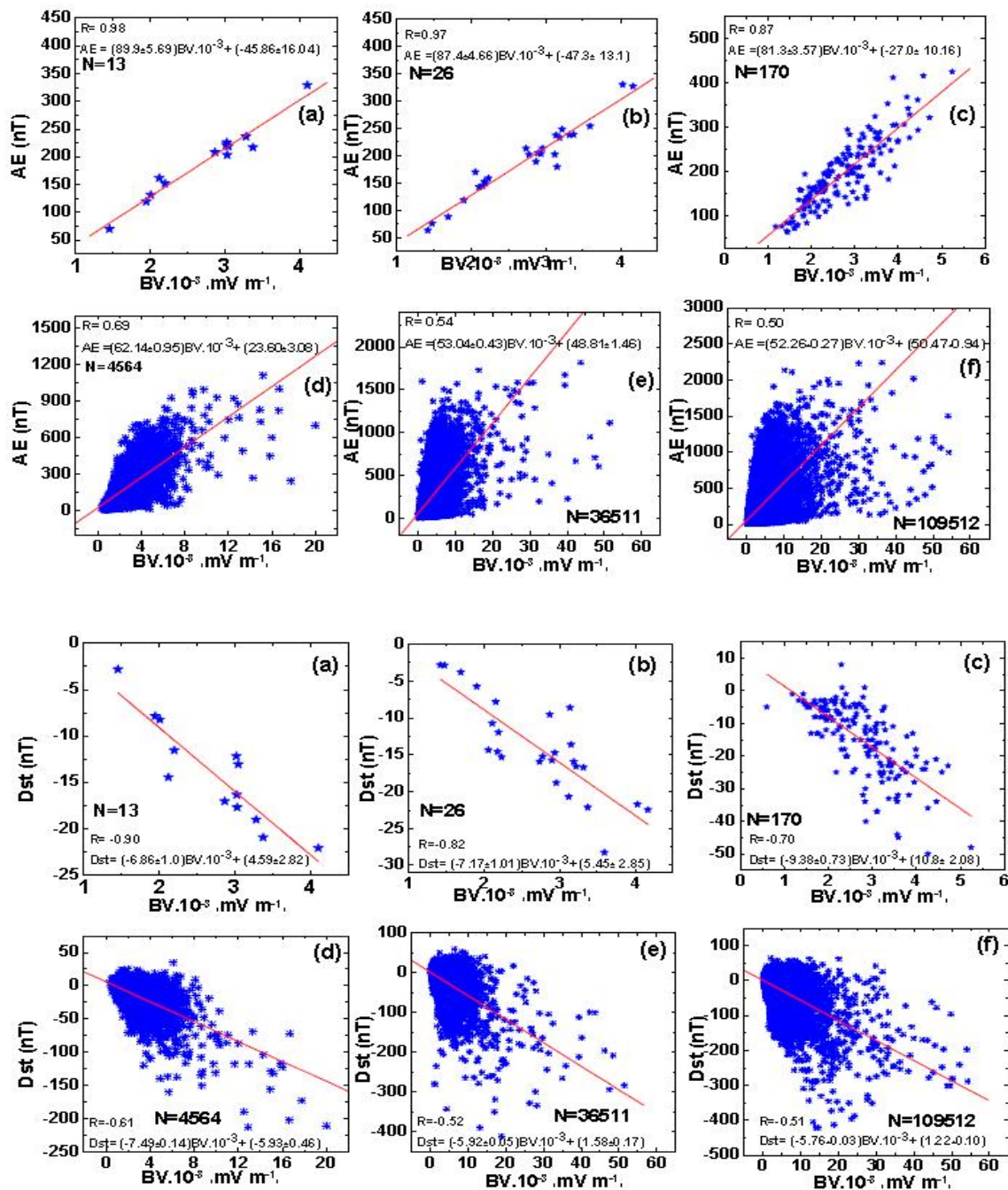


Fig. 8. (continued)

On yearly average scale, geomagnetic index ap was reported to be better correlated with V^2 than with B (Crooker et al., 1977). However, at shorter time scales Ey (BsV) or BsV^2 were suggested as preferred parameters (Burton et al., 1975; Murayama and Hakamada, 1975; Dessler and Hill, 1977). Garrett et al. (1974) suggested that on short time scales (~ 1 hour) the level of geomagnetic activity depends primarily on dawn-dusk electric field (BsV), which is proportional to V , but it is also enhanced by positive time derivative of solar wind velocity.

In addition to BsV ($-BzV$), the products BV , BV^2 , B^2V , B^2sV , BsV , BsV^2 were considered for evaluation as predictors of geomagnetic activity as measured by different geomagnetic parameters (Baker et al., 1981; Clauer et al., 1981; Holzer and Slavin, 1982). They preferred one or the other, and a physical meaning too remains unclear.

Table 3a

Linear correlation coefficient (*R*) of *ap* index with interplanetary plasma/field parameters during different phases of solar cycle 23 at different time resolutions, and for extended period (1970-2011). Best (pink) and second best (yellow) values of *R* are highlighted for each set.

Periods	Correlation coefficients (<i>R</i>)																							
	Yearly								Half yearly								27 days							
	No. of data points	B nT	Bz nT	V kms ⁻¹	Ey mVm ⁻¹	BV ² ·10 ⁻⁶ mVs ⁻¹	BzV ² ·10 ⁻⁶ mVs ⁻¹	BV ·10 ⁻³ mVm ⁻¹	No. of data points	B nT	Bz nT	V kms ⁻¹	Ey mVm ⁻¹	BV ² ·10 ⁻⁶ mVs ⁻¹	BzV ² ·10 ⁻⁶ mVs ⁻¹	BV ·10 ⁻³ mVm ⁻¹	No. of data point	B nT	Bz nT	V kms ⁻¹	Ey mVm ⁻¹	BV ² ·10 ⁻⁶ mVs ⁻¹	BzV ² ·10 ⁻⁶ mVs ⁻¹	BV ·10 ⁻³ mVm ⁻¹
Increasing including maximum (1997 Feb 7-2002 June 27)	6	0.97	0.58	0.94	-0.66	0.96	0.70	0.94	11	0.76	-0.05	0.86	-0.03	0.92	0.08	0.87	74	0.83	-0.26	0.77	0.28	0.83	-0.33	0.81
Decreasing including minimum (2002 June 28-2009 Aug 5)	7	0.88	-0.82	0.92	0.75	0.998	-0.40	0.997	15	0.93	-0.65	0.87	0.60	0.989	-0.32	0.983	96	0.67	-0.29	0.81	0.31	0.93	-0.30	0.91
Solar cycle 23 (1997 Feb 7-2009 Aug 5)	13	0.88	-0.37	0.80	0.34	0.986	-0.14	0.977	26	0.86	-0.37	0.78	0.34	0.98	-0.19	0.97	170	0.74	-0.26	0.73	0.27	0.90	-0.30	0.88
Extended period 1970-2011	42	0.85	0.02	0.70	-0.03	0.97	0.07	0.96	84	0.83	-0.05	0.72	0.06	0.96	-0.05	0.95	569	0.72	-0.13	0.70	0.16	0.88	-0.13	0.87

Correlation coefficients (R)

Periods	Correlation coefficients (R)																								
	Daily								3-Hourly								Hourly								
	No. of data points	B nT	Bz nT	V kms ⁻¹	Ey mVm ⁻¹	BV ² ·10 ⁻⁶ mVs ⁻¹	BzV ² ·10 ⁻⁶ mVs ⁻¹	BV ·10 ⁻³ mVm ⁻¹	No. of data points	B nT	Bz nT	V kms ⁻¹	Ey mVm ⁻¹	BV ² ·10 ⁻⁶ mVs ⁻¹	BzV ² ·10 ⁻⁶ mVs ⁻¹	BV ·10 ⁻³ mVm ⁻¹	No. of data point	B nT	Bz nT	V kms ⁻¹	Ey mVm ⁻¹	BV ² ·10 ⁻⁶ mVs ⁻¹	BzV ² ·10 ⁻⁶ mVs ⁻¹	BV ·10 ⁻³ mVm ⁻¹	
Increasing including maximum (1997 Feb 7-2002 June 27)	1996	0.66	-0.39	0.52	0.43	0.81	-0.40	0.81	15988	0.61	-0.41	0.43	0.44	0.69	-0.44	0.71	---	--	--	---	--	--	--	--	--
Decreasing including minimum (2002 June 28-2009 Aug 5)	2564	0.69	-0.41	0.52	0.46	0.82	-0.42	0.82	20512	0.61	-0.40	0.46	0.43	0.72	-0.40	0.73	---	--	--	---	--	--	--	--	--
Solar cycle 23 (1997 Feb 7-2009 Aug 5)	4564	0.67	-0.39	0.51	0.44	0.814	-0.40	0.82	36512	0.61	-0.40	0.44	0.43	0.71	-0.42	0.72	---	--	--	---	--	--	--	--	--
Extended period 1970-2011	15340	0.63	-0.33	0.53	0.35	0.79	-0.35	0.78	122720	0.56	-0.38	0.45	0.42	0.69	-0.42	0.69	---	--	--	---	--	--	--	--	--

Table 3b
 Linear correlation coefficient (*R*) of *aa* index with interplanetary plasma/field parameters during different phases of solar cycle 23 at different time resolutions, and for extended period (1970–2011). Best (pink) and second best (yellow) values of *R* are highlighted for each set.

Correlation coefficients (<i>R</i>)																								
Periods	Yearly								Half yearly								27 days							
	No. of data points	B	Bz	V	Ey	BV ²	BzV ²	BV	No. of data points	B	Bz	V	Ey	BV ²	BzV ²	BV	No. of data point	B	Bz	V	Ey	BV ²	BzV ²	BV
		nT	nT	kms ⁻¹	mVm ⁻¹	·10 ⁻⁶	·10 ⁻⁶	·10 ⁻³		nT	nT	kms ⁻¹	mVm ⁻¹	·10 ⁻⁶	·10 ⁻⁶	·10 ⁻³		nT	nT	kms ⁻¹	mVm ⁻¹	·10 ⁻⁶	·10 ⁻⁶	·10 ⁻³
					mVs ⁻¹	mVs ⁻¹	mVm ⁻¹						mVs ⁻¹	mVs ⁻¹	mVm ⁻¹						mVs ⁻¹	mVs ⁻¹	mVm ⁻¹	
Increasing including maximum (1997 Feb 7–2002 June 27)	6	0.88	0.60	0.95	-0.67	0.97	0.70	0.94	11	0.76	0.03	0.82	-0.05	0.93	0.09	0.88	74	0.71	-0.26	0.79	0.27	0.86	-0.33	0.84
Decreasing including minimum (2002 June 28–2009 Aug 5)	7	0.96	-0.79	0.94	0.72	0.998	-0.36	0.993	15	0.92	-0.64	0.85	0.56	0.993	-0.26	0.98	96	0.83	-0.27	0.85	0.26	0.95	-0.28	0.93
Solar cycle 23 (1997 Feb 7–2009 Aug 5)	13	0.86	-0.36	0.83	0.33	0.99	-0.12	0.97	26	0.84	-0.35	0.82	0.31	0.98	-0.15	0.96	170	0.75	-0.23	0.78	0.24	0.93	-0.27	0.90
Extended period 1970–2011	42	0.82	-0.01	0.75	-0.007	0.98	0.05	0.95	84	0.80	-0.07	0.77	0.08	0.97	-0.05	0.94	569	0.72	-0.14	0.75	0.16	0.91	-0.14	0.88

Table 3c
 Linear correlation coefficient (*R*) of *AE* index with interplanetary plasma/field parameters during different phases of solar cycle 23 at different time resolutions, and for extended period (1970-2011). Best (pink) and second best (yellow) values of *R* are highlighted for each set.

Correlation coefficients (<i>R</i>)																								
Periods	Yearly								Half yearly								27 days							
	No. of data points	B	Bz	V	Ey	BV ²	BzV ²	BV	No. of data points	B	Bz	V	Ey	BV ²	BzV ²	BV	No. of data point	B	Bz	V	Ey	BV ²	BzV ²	BV
		nT	nT	kms ⁻¹	mVm ⁻¹	·10 ⁻⁶	·10 ⁻⁶	·10 ⁻³		nT	nT	kms ⁻¹	mVm ⁻¹	·10 ⁻⁶	·10 ⁻⁶	·10 ⁻³		nT	nT	kms ⁻¹	mVm ⁻¹	·10 ⁻⁶	·10 ⁻⁶	·10 ⁻³
					mVs ⁻¹	mVs ⁻¹	mVm ⁻¹						mVs ⁻¹	mVs ⁻¹	mVm ⁻¹						mVs ⁻¹	mVs ⁻¹	mVm ⁻¹	
Increasing including maximum (1997 Feb 7-2002 June 27)	6	0.88	0.63	0.95	-0.64	0.95	0.65	0.93	11	0.66	-0.07	0.72	0.08	0.85	0.08	0.80	74	0.48	-0.31	0.77	0.33	0.73	-0.36	0.67
Decreasing including minimum (2002 June 28-2009 Aug 5)	7	0.98	-0.84	0.92	0.77	0.994	-0.44	0.999	15	0.95	-0.67	0.89	0.58	0.998	-0.29	0.992	96	0.85	-0.35	0.81	0.33	0.92	-0.35	0.92
Solar cycle 23 (1997 Feb 7-2009 Aug 5)	13	0.90	-0.43	0.77	0.40	0.97	-0.22	0.98	26	0.88	-0.41	0.77	0.37	0.96	-0.22	0.97	170	0.74	-0.30	0.72	0.30	0.87	-0.33	0.87
Extended period 1970-2011	42	0.84	-0.11	0.73	0.09	0.96	-0.04	0.95	84	0.81	-0.17	0.77	0.18	0.94	-0.04	0.93	569	0.70	-0.19	0.69	0.21	0.84	-0.19	0.83

Correlation coefficients (R)

Periods	Correlation coefficients (R)																							
	Daily								3-Hourly								Hourly							
	No. of data points	B nT	Bz nT	V kms ⁻¹	Ey mVm ⁻¹	BV ² ·10 ⁻⁶ mVs ⁻¹	BzV ² ·10 ⁻⁶ mVs ⁻¹	BV ·10 ⁻³ mVm ⁻¹	No. of data points	B nT	Bz nT	V kms ⁻¹	Ey mVm ⁻¹	BV ² ·10 ⁻⁶ mVs ⁻¹	BzV ² ·10 ⁻⁶ mVs ⁻¹	BV ·10 ⁻³ mVm ⁻¹	No. of data point	B nT	Bz nT	V kms ⁻¹	Ey mVm ⁻¹	BV ² ·10 ⁻⁶ mVs ⁻¹	BzV ² ·10 ⁻⁶ mVs ⁻¹	BV ·10 ⁻³ mVm ⁻¹
Increasing including maximum (1997 Feb 7-2002 June 27)	1996	0.52	-0.61	0.51	0.60	0.58	-0.53	0.60	15988	0.43	-0.63	0.41	0.61	0.43	-0.54	0.48	47904	0.39	-0.56	0.38	0.54	0.40	-0.47	0.44
Decreasing including minimum (2002 June 28-2009 Aug 5)	2564	0.63	-0.49	0.63	0.58	0.74	-0.45	0.76	20512	0.51	-0.54	0.52	0.52	0.56	-0.45	0.60	61632	0.47	-0.48	0.48	0.47	0.52	-0.41	0.55
Solar cycle 23 (1997 Feb 7-2009 Aug 5)	4564	0.58	-0.54	0.57	0.53	0.68	-0.48	0.69	36512	0.47	-0.58	0.46	0.56	0.51	-0.47	0.54	106512	0.43	-0.52	0.43	0.50	0.47	-0.44	0.50
Extended period 1970-2011	15340	0.53	-0.49	0.57	0.49	0.67	-0.46	0.67	122720	0.44	-0.56	0.47	0.56	0.52	-0.50	0.54	368160	0.41	-0.51	0.43	0.51	0.48	-0.46	0.50

Table 3d
 Linear correlation coefficient (R) of Dst index with interplanetary plasma/field parameters during different phases of solar cycle 23 at different time resolutions, and for extended period (1970-2011). Best (pink) and second best (yellow) values of R are highlighted for each set.

Correlation coefficients (R)																								
Periods	Yearly								Half yearly								27 days							
	No. of data points	B nT	Bz nT	V kms ⁻¹	Ey mVm ⁻¹	BV ² ·10 ⁻⁶ mVs ⁻¹	BzV ² ·10 ⁻⁶ mVs ⁻¹	BV ·10 ⁻³ mVm ⁻¹	No. of data points	B nT	Bz nT	V kms ⁻¹	Ey mVm ⁻¹	BV ² ·10 ⁻⁶ mVs ⁻¹	BzV ² ·10 ⁻⁶ mVs ⁻¹	BV ·10 ⁻³ mVm ⁻¹	No. of data point	B nT	Bz nT	V kms ⁻¹	Ey mVm ⁻¹	BV ² ·10 ⁻⁶ mVs ⁻¹	BzV ² ·10 ⁻⁶ mVs ⁻¹	BV ·10 ⁻³ mVm ⁻¹
Increasing including maximum (1997 Feb 7-2002 June 27)	6	-0.67	-0.35	-0.46	0.49	-0.61	-0.61	-0.63	11	-0.40	0.35	-0.72	-0.26	-0.46	0.16	-0.43	74	-0.54	0.43	-0.41	-0.42	-0.55	0.46	-0.56
Decreasing including minimum (2002 June 28-2009 Aug 5)	7	-0.93	0.73	-0.93	-0.64	-0.97	0.31	-0.96	15	-0.88	0.55	-0.87	-0.49	-0.84	0.29	-0.87	96	-0.81	0.34	-0.57	-0.32	-0.75	0.30	-0.80
Solar cycle 23 (1997 Feb 7-2009 Aug 5)	13	-0.92	0.42	-0.54	-0.34	-0.83	0.12	-0.90	26	-0.82	0.44	-0.52	-0.39	-0.77	0.24	-0.82	170	-0.68	0.39	-0.44	-0.37	-0.66	0.39	-0.70
Extended period 1970-2011	42	-0.85	-0.003	-0.33	0.05	-0.76	-0.09	-0.83	84	-0.78	0.13	-0.42	-0.12	-0.76	0.10	-0.80	569	-0.65	0.21	-0.46	-0.20	-0.68	0.19	-0.71

Correlation coefficients (R)

Periods	Daily							3-Hourly							Hourly									
	No. of data points	B nT	Bz nT	V kms ⁻¹	Ey mVm ⁻¹	BV ² ·10 ⁻⁶ mVs ⁻¹	BzV ² ·10 ⁻⁶ mVs ⁻¹	BV ·10 ⁻³ mVm ⁻¹	No. of data points	B nT	Bz nT	V kms ⁻¹	Ey mVm ⁻¹	BV ² ·10 ⁻⁶ mVs ⁻¹	BzV ² ·10 ⁻⁶ mVs ⁻¹	BV ·10 ⁻³ mVm ⁻¹	No. of data point	B nT	Bz nT	V kms ⁻¹	Ey mVm ⁻¹	BV ² ·10 ⁻⁶ mVs ⁻¹	BzV ² ·10 ⁻⁶ mVs ⁻¹	BV ·10 ⁻³ mVm ⁻¹
	Increasing including maximum (1997 Feb 7-2002 June 27)	1996	-0.46	0.39	-0.48	-0.36	-0.61	0.29	-0.59	15988	-0.40	0.32	-0.45	-0.30	-0.49	0.25	-0.49	47904	-0.38	0.29	-0.44	-0.27	-0.48	0.22
Decreasing including minimum (2002 June 28-2009 Aug 5)	2564	-0.51	0.45	-0.51	-0.45	-0.64	0.41	-0.64	20512	-0.43	0.36	-0.47	-0.36	-0.56	0.31	-0.55	61632	-0.42	0.31	-0.47	-0.31	-0.54	0.26	-0.64
Solar cycle 23 (1997 Feb 7-2009 Aug 5)	4564	-0.49	0.42	-0.47	-0.40	-0.62	0.35	-0.61	36512	-0.42	0.34	-0.44	-0.33	-0.53	0.28	-0.52	106512	-0.41	0.30	-0.43	-0.29	-0.51	0.24	-0.60
Extended period 1970-2011	15340	-0.43	0.38	-0.48	-0.36	-0.59	0.34	-0.58	122720	-0.6	0.33	-0.44	-0.33	-0.51	0.30	-0.49	368160	-0.35	0.29	-0.44	-0.29	-0.49	0.25	-0.48

Table 4
 Best-fit linear equation and correlation coefficients between geomagnetic parameters and BV (mV m^{-1}), BV^2 (mV s^{-1}) at different time resolutions

Geomagnetic parameters	Yearly		6-monthly		27-day		Daily		3-hourly		Hourly	
	Relation	R	Relation	R	Relation	R	Relation	R	Relation	R	Relation	R
$ap =$	$9.88(BV^2 \cdot 10^{-6}) - 1.20$	0.99	$9.89(BV^2 \cdot 10^{-6}) - 1.20$	0.98	$10.72(BV^2 \cdot 10^{-6}) - 1.36$	0.90	$10.15(BV^2 \cdot 10^{-6}) - 1.56$	0.82	$8.91(BV^2 \cdot 10^{-6}) - 0.17$	0.71	--	--
	$6.02(BV \cdot 10^{-3}) - 4.88$	0.98	$6.06(BV \cdot 10^{-3}) - 4.98$	0.97	$6.40(BV \cdot 10^{-3}) - 5.62$	0.88	$6.96(BV \cdot 10^{-3}) - 7.52$	0.82	$6.59(BV \cdot 10^{-3}) - 6.54$	0.72		
$aa =$	$15.15(BV^2 \cdot 10^{-6}) + 1.00$	0.99	$15.12(BV^2 \cdot 10^{-6}) + 1.04$	0.98	$15.97(BV^2 \cdot 10^{-6}) + 1.24$	0.93	$13.62(BV^2 \cdot 10^{-6}) + 2.98$	0.80	$11.58(BV^2 \cdot 10^{-6}) + 5.45$	0.68	--	--
	$9.13(BV \cdot 10^{-3}) - 4.36$	0.97	$9.18(BV \cdot 10^{-3}) - 4.50$	0.96	$9.46(BV \cdot 10^{-3}) - 4.91$	0.90	$9.41(BV \cdot 10^{-3}) - 5.19$	0.81	$8.69(BV \cdot 10^{-3}) - 3.17$	0.70		
$AE =$	$140.12(BV^2 \cdot 10^{-6}) + 10.49$	0.97	$140.0(BV^2 \cdot 10^{-6}) + 10.60$	0.96	$131.8(BV^2 \cdot 10^{-6}) + 33.1$	0.87	$88.21(BV^2 \cdot 10^{-6}) + 79.80$	0.68	$68.20(BV^2 \cdot 10^{-6}) + 105.0$	0.51	$67.43(BV^2 \cdot 10^{-6}) + 105.88$	0.47
	$89.9(BV \cdot 10^{-3}) - 45.86$	0.98	$87.4(BV \cdot 10^{-3}) - 47.3$	0.97	$81.3(BV \cdot 10^{-3}) - 27.0$	0.87	$62.14(BV \cdot 10^{-3}) + 23.6$	0.69	$53.04(BV \cdot 10^{-3}) + 48.81$	0.54	$52.26(BV \cdot 10^{-3}) + 50.47$	0.50
$Dst =$	$-10.26(BV^2 \cdot 10^{-6}) - 0.88$	-0.83	$-10.76(BV^2 \cdot 10^{-6}) - 0.23$	-0.77	$-14.48(BV^2 \cdot 10^{-6}) + 3.01$	-0.66	$-10.99(BV^2 \cdot 10^{-6}) - 0.37$	-0.62	$-8.21(BV^2 \cdot 10^{-6}) - 3.87$	-0.53	$-7.97(BV^2 \cdot 10^{-6}) - 4.16$	-0.51
	$-6.86(BV \cdot 10^{-3}) + 4.59$	-0.90	$-7.17(BV \cdot 10^{-3}) + 5.45$	-0.82	$-9.38(BV \cdot 10^{-3}) + 10.8$	-0.70	$-7.49(BV \cdot 10^{-3}) - 5.93$	-0.61	$-5.92(BV \cdot 10^{-3}) + 1.58$	-0.51	$-5.76(BV \cdot 10^{-3}) + 1.22$	-0.51

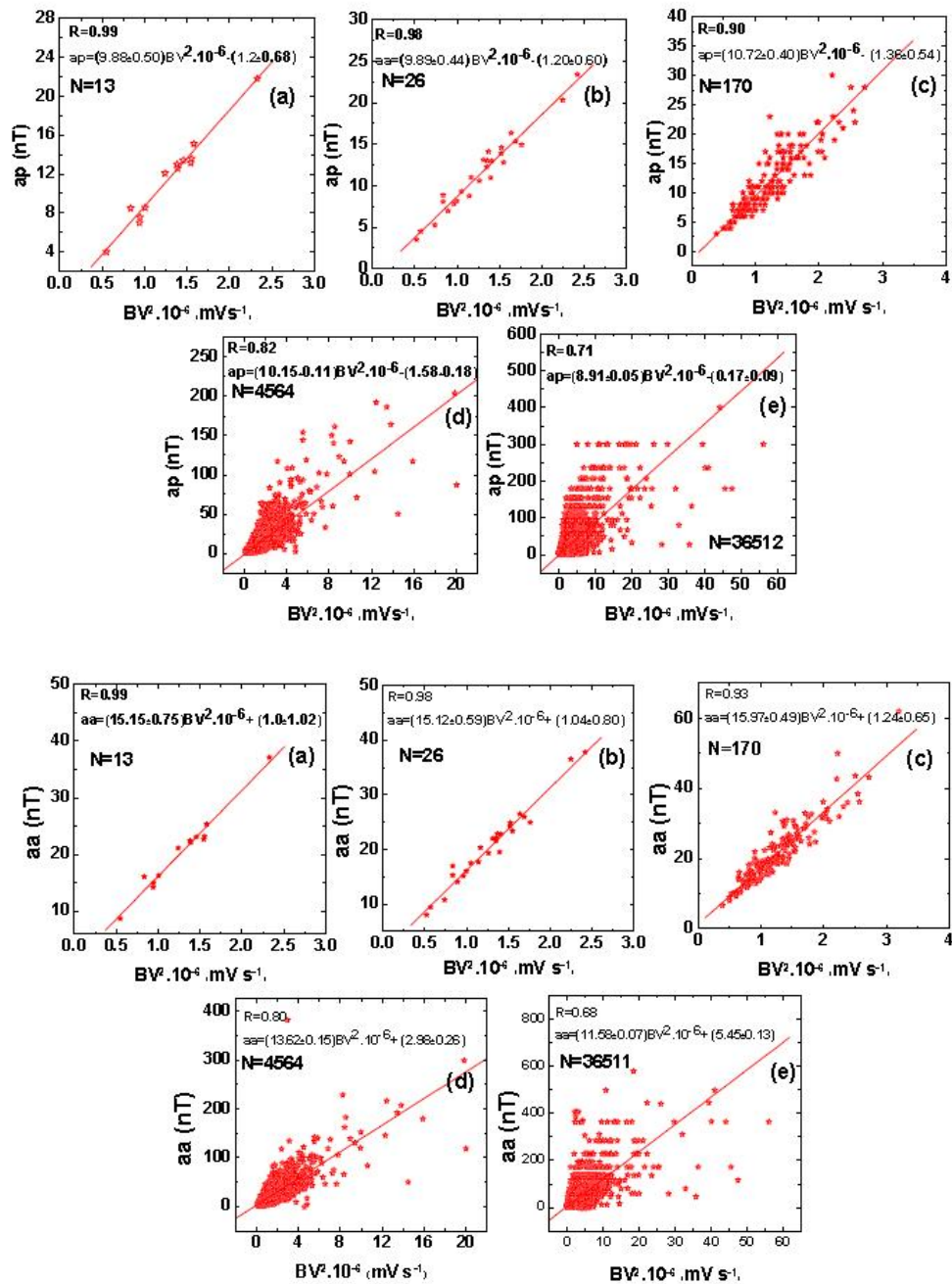


Fig. 9. (A) Scatter plot and best-fit linear curve between geomagnetic index ap and BV^2 at different time resolutions; (a) yearly, (b) half-yearly, (c) 27-day, (d) daily and (e) 3-hourly. (B) Scatter plot and best fit linear curve between geomagnetic index aa and BV^2 at different time resolutions; (a) yearly, (b) half-yearly, (c) 27-day, (d) daily and (e) 3-hourly. (C) Scatter plot and best-fit linear curve between geomagnetic index AE and BV^2 at different time resolutions; (a) yearly, (b) half-yearly, (c) 27-day, (d) daily, (e) 3-hourly and (f) hourly. (D) Scatter plot and best-fit linear curve between geomagnetic index Dst and BV^2 at different time resolutions; (a) yearly, (b) half-yearly, (c) 27-day, (d) daily, (e) 3-hourly and (f) hourly.

Using 27-day average data (1964-1999), Papitashvili et al. (2000) have revealed that over long time scales, the total interplanetary electric field ($E = BV$), in which the magnetic sphere is immersed, plays a significant role in driving global geomagnetic activity. Sabbah (2000) used yearly average geomagnetic and interplanetary data for the period 1978-1995 and reached at the conclusion that the product BV directly modulates the geomagnetic activity and that this product (BV) is more important for the geomagnetic activity modulation rather than the interplanetary magnetic field alone.

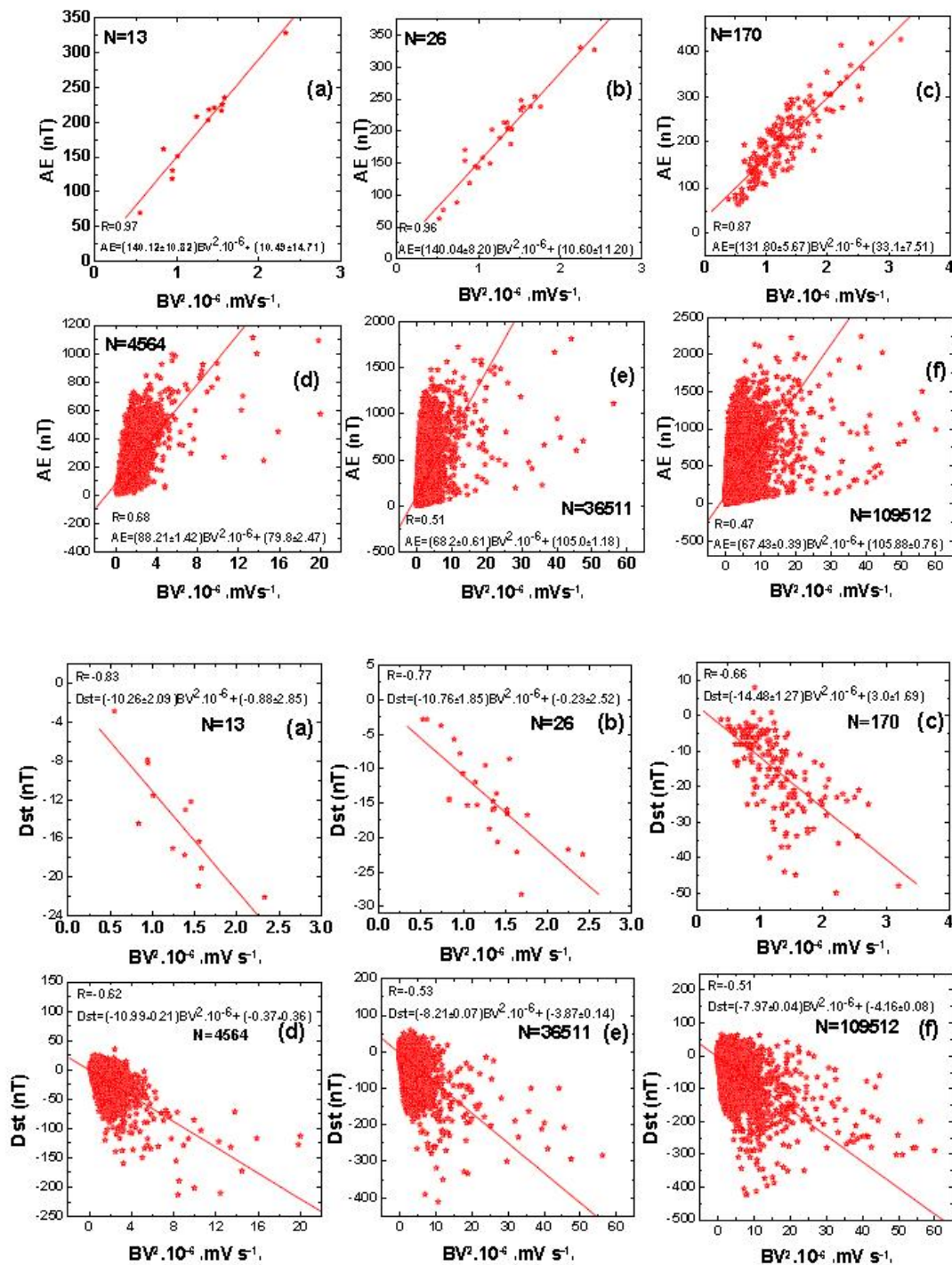


Fig. 9. (continued)

Two parameters that appears most in relation with geomagnetic indices are $-Bz$ (B_s) and V (their product B_sV also). However, there is consider scatter in $-Dst(\min)$ at low $-Bz$ values (< 20 nT). Even at considerably large $-Bz$ and E_y ($-BzV$), $-Dst(\min)$ range is considerably large (see Kane, 2010; Singh and Badruddin, 2012). It is very likely that some interplanetary parameter(s)/conditions may play a role in enhancing the geomagnetic activity under similar $-Bz$ and/or E_y conditions. We suggest that fluctuations in interplanetary electric potential in space [interplanetary electric field $BV/1000$ (mV m^{-1})] and/or time [BV^2 (mV s^{-1})] are likely to influence the reconnection rate at the magnetopause to a certain extent when

interplanetary field orientation is favourable for reconnection. We suspect that faster variation (spacial and/or time) in interplanetary electric potential might enhance the reconnection rate and increase the amount of energy transfer from the solar wind into the magnetosphere.

3. Conclusions

The spacial and/or time variability of interplanetary electric potential (BV , BV^2) at the magnetopause appears to be an important parameter for solar wind-magnetosphere coupling. When one or both of these variabilities in interplanetary potential are sufficiently large, it is likely to increase the reconnection rate between the solar wind and terrestrial magnetosphere, significantly increasing the geoefficiency of the solar wind.

It is thought that the principal manifestation of geomagnetic storms, measured by Dst , is the increase in the ring current intensity, which depends upon the reconnection rate (between the solar wind and the magnetosphere) that allows the solar wind energy transfer into the Earth's magnetosphere/magneto-tail. It is generally believed that a persistent southward IMF ($-Bz$) produces increased geomagnetic activity, and dawn-dusk electric field ($-VxBz$) is a crucial storm parameter. We suspect that, although the duskward electric field is responsible for initiating the geomagnetic disturbances, the enhanced spacial and/or time fluctuations in the interplanetary electric potential at near the magnetopause is/are the likely additional effect(s) that lead to enhanced coupling between the solar wind and the terrestrial magnetosphere, significantly increasing the geoeffectiveness of the solar wind. However, exact role and mechanism that involves these parameters needs to be identified. We put forward the idea that, when the interplanetary potential at/near the magnetopause fluctuates, in space and/or time, at a sufficiently fast rate, under southward Bz conditions, it appears to enhance the reconnection rate at the magnetopause. This in turn may cause faster magnetic merging, that occur leading to energy transfer at an enhanced rate from the solar wind to the magnetosphere. However, this hypothesis needs to be tested with high time resolution in situ measurements of interplanetary data. If confirmed, our hypothesis has important implications for solar-terrestrial physics and space weather forecast.

Acknowledgements

We gratefully acknowledge the availability of solar, geomagnetic and solar wind plasma/field data through the NASA/GSFC OMNI Web interface and National Geophysical Data Center. We also thank the reviewer, whose comments and suggestions helped us to improve the paper.

References

- Akasofu, S. -I., 1981. Energy coupling between the solar wind and the magnetosphere. *Space Science Reviews* 28, 121-190.
- Alves, M. V., Echer, E., Gonzalez, W. D., 2011. Geoeffectiveness of solar wind interplanetary magnetic structures. *Journal of Atmospheric and Solar-Terrestrial Physics* 73, 1380-1384.
- Arnoldy, R. L., 1971. Signature in the interplanetary medium for substorms. *Journal of Geophysical Research* 76, 5189-5201.
- Badruddin, 1998. Interplanetary shocks, magnetic clouds, stream interfaces and resulting geomagnetic disturbances. *Planetary and Space Science* 46, 1015-1028.
- Badruddin, Singh, Y. P., 2009. Geoeffectiveness of magnetic cloud, shock/sheath, interaction region, high-speed stream and their combined occurrence. *Planetary and Space Science* 57, 318-331.
- Baker, D. N., Hones, E. W. Jr., Payne, J. B., Fedman, W. C., 1981. A high time resolution study of interplanetary parameter correlations with AE . *Geophysical Research Letters* 8, 179-183.
- Boudouridis, A., Zesta, E., Lyons, L. R., Anderson, P. C., Lummerzheim, D., 2005. Enhanced solar wind geoeffectiveness after a sudden increase in dynamic pressure during southward IMF orientation. *Journal of Geophysical Research* 110, A05214.
- Burton, R. K., McPherron, R. L., Russel, C. T., 1975. An empirical relationship between interplanetary conditions and Dst . *Journal of Geophysical Research* 80, 4204-4214.
- Clauer, C. R., McPherron, R. L., Searls, C., Kievson, M.G., 1981. Solar wind control of auroral zone geomagnetic activity. *Geophysical Research Letters* 8, 915-918.
- Crooker, N. U., Feynman, J., Gosling, J. T., 1977. On the high correlation between long-term averages of solar wind speed and geomagnetic activity. *Journal of Geophysical Research* 82, 1933-1937.

- Dessler, A. J., Fejer, J. A., 1963. Interpretation of *Kp* index and M-region geomagnetic storms. *Planetary and Space Science* 11, 505-511.
- Dessler, A. J., Hill, T. W., 1977. Comment on "On the high correlation between long-term averages of solar wind speed and geomagnetic activity" by Crooker, N. U., Feynman, J., Gosling, J. T. *Journal of Geophysical Research* 82, 5644.
- Dungey, J. W., 1961. Interplanetary Magnetic Field and the Auroral Zones. *Physical Review Letters* 6, 47-48.
- Dwivedi, V. C., Tiwari, D. P., Agrawal, S. P., 2009. Study of the long-term variability of interplanetary plasma and fields as a link for solar-terrestrial relationships. *Journal of Geophysical Research* 114, A05108.
- Echer, E., Alves, M. V., Gonzalez, W. D., 2005. A statistical study of magnetic cloud parameters and geoeffectiveness. *Journal of Atmospheric and Solar-Terrestrial Physics* 67, 839-852.
- Garrett, H. B., Dessler, A. J., Hill, T. W., 1974. Influence of solar wind variability on geomagnetic activity. *Journal of Geophysical Research* 79, 4603-4610.
- Gopalswamy, N., Yashiro, S., Akiyama, S., 2007. Geoeffectiveness of halo coronal mass ejections. *Journal of Geophysical Research* 112, A06112.
- Gopalswamy, N., Akiyama, S., Yashiro, S., Michalek, G., Lepping, R. P., 2008. Solar sources and geospace consequences of interplanetary magnetic clouds observed during solar cycle 23. *Journal of Atmospheric and Solar-Terrestrial Physics* 70, 245-253.
- Guo, J., Feng, X., Emery, B. A., Zhang, J., Xiang, C., Shen, F., Song, W., 2011. Energy transfer during intense geomagnetic storms driven by interplanetary coronal mass ejections and their sheath regions. *Journal of Geophysical Research* 116, A05106.
- Gupta, V., Badruddin, 2009. Interplanetary structures and solar wind behaviour during major geomagnetic perturbations. *Journal of Atmospheric and Solar-Terrestrial Physics* 71, 885-896.
- Holzer, R. E., Slavin, J. A., 1979. A correlative study of magnetic flux transfer in the magnetosphere. *Journal of Geophysical Research* 84, 2573-2578.
- Holzer, R. E., Slavin, J. A., 1982. An evaluation of three predictors of geomagnetic activity. *Journal of Geophysical Research* 87, 2558-2562.
- Joshi, N. L., Bankoti, N. S., Pande, S., Pande, B., Pandey, K., 2011. Relationship between interplanetary field/plasma parameters with geomagnetic indices and their behavior during intense geomagnetic storms. *New Astronomy* 16, 366-385.
- Kane, R. P., 2010. Relationship between the geomagnetic *Dst*(min) and the interplanetary *Bz*(min) during cycle 23. *Planetary and Space Science* 58, 392-400.
- Kershengolts, S. Z., Barkova, E. S., Plotnikov, I. Ya., 2007. Dependence of geomagnetic disturbances on extreme values of the solar wind *Ey* component. *Geomagnetism and Aeronomy* 47, 156-164.
- Kim, R. S., Cho, K. S., Moon, Y. J., Kim, Y. H., Yi, Y., Dryer, M., Bong, S.-C., Park, Y.-D., 2005. Forecast evaluation of the coronal mass ejection (CME) geoeffectiveness using halo CMEs from 1997 to 2003. *Journal of Geophysical Research* 110, A11104.
- Kudela, K., 2013. Space weather near Earth and energetic particles: selected results. *Journal of Physics: Conference Series* 409, 012017 (1-14).
- Kudela, K., Storini, M., 2005. Cosmic ray variability and geomagnetic activity: A statistical study. *Journal of Atmospheric and Solar-Terrestrial Physics* 67, 907-912.
- Lepping, R. P., Burlaga, L. F., Tsurutani, B. T., Ogilvie, K. W., Lazarus, A. J., Evans, D., Klein, L. W., 1991. The interaction of a very large interplanetary magnetic cloud with the magnetosphere and with cosmic rays. *Journal of Geophysical Research* 96, 9425-9438.
- März, F., 1992. Geomagnetic, ionospheric and cosmic ray variations around the passages of different magnetic clouds. *Planetary and Space Science* 40, 979-983.
- Murayama, T., 1982. Coupling function between solar wind parameters and geomagnetic indices. *Reviews of Geophysics and Space Physics* 20, 623-629.
- Murayama, T., Hakamada, K., 1975. Effects of solar wind parameters on the development of magnetospheric substorms. *Planetary and Space Science* 23, 75-91.
- Mustajab, F., Badruddin, 2011. Geoeffectiveness of the interplanetary manifestations of coronal mass ejections and solar-wind stream-stream interactions. *Astrophysics and Space Science* 331, 91-104.
- Ontiveros, V., Gonzalez-Esparza, J. A., 2010. Geomagnetic storms caused by shocks and ICMEs. *Journal of Geophysical Research* 115, A10244.
- Papitashvili, V. O., Papitashvili, N. E., King, J. H., 2000. Solar cycle effects in planetary geomagnetic activity: Analysis of 36-year long OMNI dataset. *Geophysical Research Letters* 27, 2797-2800.
- Richardson, I. G., Cane, H. V., 2011. Geoeffectiveness (*Dst* and *Kp*) of interplanetary coronal mass ejections during 1995-2009 and implications for storm forecasting. *Space Weather* 9, S07005.
- Richardson, I. G., Cliver, E. W., Cane, H. V., 2000. Sources of geomagnetic activity over the solar cycle: Relative importance of coronal mass ejections, high-speed streams, and slow solar wind. *Journal of Geophysical Research* 105, 18203-18213.
- Rossberg, L., 1989. The effect of solar wind velocity on substorm activity. *Journal of Geophysical Research* 94, 13571-13574.

- Rostoker, G., Fälthammar, C. -G., 1967. Relationship between changes in the interplanetary magnetic field and variations in the magnetic field at the Earth's surface. *Journal of Geophysical Research* 72, 5853-5863.
- Sabbah, I., 2000. The role of interplanetary magnetic field and solar wind in modulating both galactic cosmic rays and geomagnetic activity. *Geophysical Research Letters* 27, 1823-1826.
- Singh, Y. P., Badruddin, 2007. Effects of interplanetary magnetic clouds, interaction regions, and high-speed streams on the transient modulation of galactic cosmic rays. *Journal of Geophysical Research* 112, A02101.
- Singh, Y. P., Badruddin, 2012. Study of the influence of magnetic fluctuations and solar plasma density on the solar wind-magnetosphere coupling. *Journal of Atmospheric and Solar-Terrestrial Physics* 75, 15-21.
- Snyder, C. W., Neugebauer, M., Rao, U. R., 1963. The solar wind velocity and its correlation with cosmic rays variations and with solar and geomagnetic activity. *Journal of Geophysical Research* 68, 6361-6370.
- Srivastava, N., Venkatakrishnan, P., 2002. Relationship between CME Speed and Geomagnetic Storm Intensity. *Geophysical Research Letters* 29(9), 1287.
- Tsurutani, B. T., Gonzalez, W. D., 1997. The Interplanetary causes of magnetic storms: A review. In: Tsurutani, B. T., Gonzalez, W. D., Kamide, Y. (Eds.), *Magnetic Storms*. (1997), *Geophysical Monograph Series* 98, AGU, Washington DC, 77-89.
- Webb, D. F., Cliver, E. W., Crooker, N. U., St.Cyr. O. C., Thompson, B. J., 2000. Relationship of halo coronal mass ejections, magnetic clouds, and magnetic storms. *Journal of Geophysical Research* 105, 7491-7508.
- Xie, H., Gopalswamy, N., St.Cyr, O. C., Yashiro, S., 2008. Effects of solar wind dynamic pressure and preconditioning on large geomagnetic storms. *Geophysical Research Letters* 35, L06S08.
- Yermolaev, Y. I., Nikolaeva, N. S., Lodkina, I. G., Yermolaev, M. Y., 2010. Relative occurrence rate and geoeffectiveness of large-scale types of the solar wind. *Cosmic Research* 48, 1-30.
- Yermolaev, Y. I., Nikolaeva, N. S., Lodkina, I. G., Yermolaev, M. Y., 2012. Geoeffectiveness and efficiency of CIR, sheath, and ICME in generation of magnetic storms. *Journal of Geophysical Research* 117, A00L07.
- Zhang, G., Burlaga, L. F., 1988. Magnetic clouds, geomagnetic disturbances, and cosmic ray decreases. *Journal of Geophysical Research* 93, 2511-2518.
- Zhang, J., Richardson, I. G., Webb, D. F., Gopalswamy, N., Huttunen, E., Kasper, J. C., Nitta, N. V., Poomvises, W., Thompson, B. J., Wu, C.-C., Yashro, S., Zhukov, A. N., 2007. Solar and interplanetary sources of major geomagnetic storms ($Dst \leq -100nT$) during 1996-2005. *Journal of Geophysical Research* 112, A10102.